medRxiv preprint doi: https://doi.org/10.1101/2020.11.30.20241174; this version posted December 2, 2020. The copyright holder for this preprint (which was not certified by peer review) is the author/funder, who has granted medRxiv a license to display the preprint in perpetuity. It is made available under a CC-BY-NC-ND 4.0 International license .

Modeling the effectiveness of olfactory testing to limit SARS-2-CoV transmission

Daniel B. Larremore[1,2], Derek Toomre[3], and Roy Parker[2,4,5]

[1]*Department of Computer Science, University of Colorado Boulder*
[2]*BioFrontiers Institute, University of Colorado Boulder*
[3]*Department of Cell Biology, Yale University School of Medicine*
[4]*Department of Biochemistry, University of Colorado Boulder*
[5]*Howard Hughes Medical Institute*

Abstract

A central problem in the COVID-19 pandemic is that there is not enough testing to prevent infectious spread of SARS-CoV-2, causing surges and lockdowns with human and economic toll. Molecular tests that detect viral RNAs or antigens will be unable to rise to this challenge unless testing capacity increases by at least an order of magnitude while decreasing turnaround times. Here, we evaluate an alternative strategy based on the monitoring of olfactory dysfunction, a symptom identified in 76-83% of SARS-CoV-2 infections—including those that are otherwise asymptomatic—when a standardized olfaction test is used. We model how screening for olfactory dysfunction, with reflexive molecular tests, could be beneficial in reducing community spread of SARS-CoV-2 by varying testing frequency and the prevalence, duration, and onset time of olfactory dysfunction. We find that monitoring olfactory dysfunction could reduce spread via regular screening, and could reduce risk when used at point-of-entry for single-day events. In light of these estimated impacts, and because olfactory tests can be mass produced at low cost and self-administered, we suggest that screening for olfactory dysfunction could be a high impact and cost effective method for broad COVID-19 screening and surveillance.

To whom correspondence should be addressed:
daniel.larremore@colorado.edu, derek.toomre@yale.edu, roy.parker@colorado.edu

NOTE: This preprint reports new research that has not been certified by peer review and should not be used to guide clinical practice.

medRxiv preprint doi: https://doi.org/10.1101/2020.11.30.20241174; this version posted December 2, 2020. The copyright holder for this preprint (which was not certified by peer review) is the author/funder, who has granted medRxiv a license to display the preprint in perpetuity. It is made available under a CC-BY-NC-ND 4.0 International license .

Introduction

The COVID-19 pandemic has created a global public health crisis. Due to the fact that SARS-CoV-2 can spread from individuals with and without overt symptoms [1–3], there remains an urgent need to identify infected individuals prior to onward spread. To meet this need, large efforts are currently underway to develop, regulate, and mass produce rapid, inexpensive, and effective screening tests for viral antigens that could be used repeatedly and at wide scale. However, an alternative approach is to utilize widespread screening of symptoms of SARS-2-CoV infection, which could then stratify individuals with symptoms for follow-up molecular testing. Unfortunately, fever, an overt and easily identified symptom of COVID-19, does not have the qualities necessary to be an effective screening symptom.

Fever was advanced early in the pandemic as a potential screening symptom but failed [4] because fever ($\geq$38°C) is (i) only present in 18-26% of COVID-19 cases [5–7], (ii) occurs in many diseases (e.g. Flu) and is not specific to COVID-19 [8], and (iii) lasts only 1.5 days on average [5]. Nevertheless, temperature checks persist at many hospital entrances due to the speed and convenience of contactless thermometers and thermography.

In contrast to fever, several observations indicate that olfactory dysfunction—hyposmia or anosmia—may be a superior screening symptom. First, although the prevalence of olfactory dysfunction associated with SARS-CoV-2 was moderate in a meta-analysis of self-report surveys (41-53%), it increased to 76-83% as soon as a standardized olfactory dysfunction test was performed [9, 10], including 82% of individuals who were otherwise entirely asymptomatic [11]. This demonstrates that screening for olfactory dysfunction will require a standardized olfactory test. Second, olfactory dysfunction is much more specific to COVID-19, with an odds ratio of 10.4, a 4-10-fold higher association with COVID-19 than fever [12], and no association with influenza[1]. Third, onset of anosmia may precede overt symptoms (e.g. difficulty breathing, cough, and diarrhea) by days [13–20]. Fourth, COVID-induced olfactory dysfunction has been shown to last roughly 7 days in clinical studies [9, 10, 14, 21]. Combined, olfactory dysfunction's prevalence, specificity, onset time, and duration have led us to hypothesize that, while it is not an overt symptom of COVID-19 and is underreported in self-reporting surveys [9, 10], standardized olfactory dysfunction testing may be a valuable but underutilized screening tool.

Recent modeling work has shown that, for COVID-19 screening via repeated molecular testing, test frequency and turnaround time are critical, while test sensitivity is secondary [22, 23]. Standardized olfactory dysfunction testing may be sufficiently low cost to be performed frequently, and olfactory dysfunction testing can be self-administered in minutes without personal protective equipment (PPE). We therefore considered whether olfactory dysfunction could be effectively used in a similar repeated regimen to proposed molecular testing [22, 24], and to what extent its effectiveness depends on its onset time, duration, and prevalence among those who are infected but do not experience overt COVID-19 symptoms.

Methods summary

We analyzed how screening for olfactory dysfunction could impact COVID-19 spread while varying the prevalence of olfactory dysfunction among infected individuals, its duration, the timing of onset, and the frequency of testing. In each case we analyzed the impact of screening regimens in two manners.

In one set of analyses, we used a simple fully-mixed Susceptible-Exposed-Infectious-Recovered (SEIR)

[1] https://www.cdc.gov/flu/symptoms/flu-vs-covid19.htm

medRxiv preprint doi: https://doi.org/10.1101/2020.11.30.20241174; this version posted December 2, 2020. The copyright holder for this preprint (which was not certified by peer review) is the author/funder, who has granted medRxiv a license to display the preprint in perpetuity. It is made available under a CC-BY-NC-ND 4.0 International license .

model representing a population of 20,000 people, similar to a large university setting, with a constant rate of external infection approximately equal to one new import per day [22]. Individual viral loads were simulated for each infection based on key features of latency, proliferation, peak, and clearance identified in the literature (Materials and Methods; [22, 25]). Infected individuals who scored positive for olfactory dysfunction were considered to be tested for SARS-CoV-2 by RT-PCR and were isolated if positive. To better model viral dynamics and behavior in the presence of overt and noticeable symptoms, 35% of modeled individuals had viral load trajectories with prolonged clearance times [25, 26], and were modeled to self-isolate within 0-2 days of peak viral load, independent of screening-related testing. Contact tracing was not included to more conservatively estimate the impacts of screening alone [27, 28]. We used a value of R_0 of 1.6, to reflect accelerating but partially mitigated transmission.

In a second set of analyses, we simulated the viral loads, possible onset of olfactory dysfunction, and infectiousness curves, of 10,000 individuals and then examined how much infectiousness was removed from the population by different olfaction testing regimens. This allowed us to examine the results of modeling under a range of different screening strategies and olfactory dysfunction parameters by estimating the impact, in each case, on the reproductive number R.

In all analyses, we considered 80% of the population to participate in the screening protocol, examined performing olfactory testing either daily, every third day, or weekly, and infectiousness was taken to be proportional to the logarithm of viral load in excess of 10^6 virions/ml [22]. We modeled that 4% of individuals would have a COVID-19-independent olfactory dysfunction [29–31]. Details of both models and parameters are fully described in Materials and Methods.

Results

Olfactory dysfunction screening can impact population spread

We first examined how the prevalence of olfactory dysfunction during COVID-19 infection would impact its use in a screening regimen. Olfactory dysfunction has been suggested to occur in 50-90% of COVID-19 infections for roughly one week [9, 10, 14, 21]. Thus, we modeled olfactory dysfunction as a symptom able to be detected with an olfactory test in 25% (underestimate), 50% (low estimate), 75% (realistic), and 90% (high estimate) of infected individuals with a duration of 7 days [14, 21]. Although reports indicate that olfactory dysfunction is an early COVID-19 symptom [13–20], the precise timing of olfactory dysfunction relative to viral loads is unclear. Given this uncertainty, we initially modeled the average onset of olfactory dysfunction as occurring one day after viral loads reached detectable levels based on RT-PCR, consistent with studies indicating that onset of olfactory dysfunction precedes onset of overt symptoms [13–20].

We observed that screening for olfactory dysfunction daily (Fig. S1A) or every third day (Fig. 1A) prevented outbreaks in simulations, provided symptom prevalence was 50% or greater. Notably, when symptom prevalence was 75% or higher olfactory screening every third day was more effective than weekly RT-PCR testing with a one-day turnaround time (Fig. 1; yellow dashed line). At 50% symptom prevalence, viral spread was partially controlled by testing every three days (Fig. 1), and more effectively controlled with daily testing (Fig. S1A). Weekly olfactory screening mitigated but failed to fully control outbreaks except when symptom prevalence was modeled at 90% (Fig. S1B).

By estimating the reduction in the reproductive number R for each scenario, we were able to perform direct comparisons of the predicted effectiveness of screening strategies across transmission scenarios (Fig. 1B).

medRxiv preprint doi: https://doi.org/10.1101/2020.11.30.20241174; this version posted December 2, 2020. The copyright holder for this preprint (which was not certified by peer review) is the author/funder, who has granted medRxiv a license to display the preprint in perpetuity. It is made available under a CC-BY-NC-ND 4.0 International license .

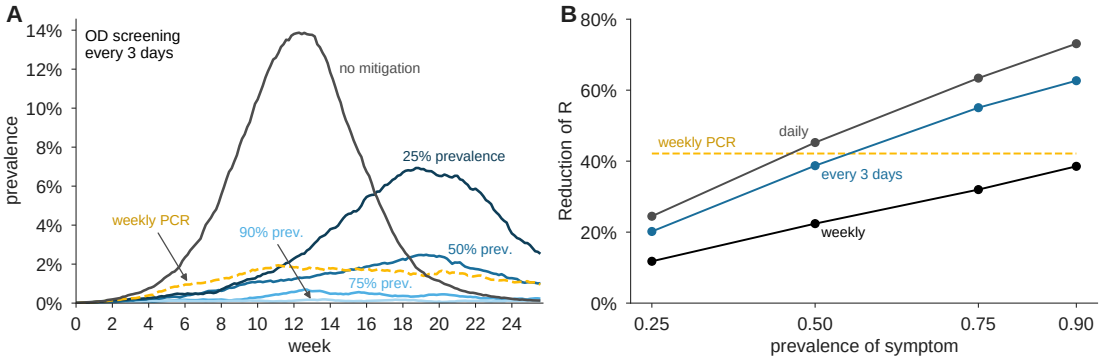

Figure 1: **Impact of olfactory dysfunction prevalence on its effectiveness to limit viral spread.** (A) Examples of viral spread in a community of 20,000 individuals performing olfactory dysfunction (OD) screening every three days. No mitigation (black), Prevalence of symptom shown are: 25% (dark blue), 50% (medium blue), 75% (light blue), 90% (lightest blue). For comparison, weekly RT-PCR testing with a one-day turnaround is shown (yellow). In this analysis, olfactory dysfunction is modeled to last 7 days and begin one day after viral levels reach ∼1000 virions/ml. (B) Reduction of reproductive number R with different testing regimens showing the impact of symptom prevalence with weekly (black line), every three days (blue line), or daily (gray line), testing for olfactory dysfunction. Weekly RT-PCR testing is shown for comparison (yellow dashed line). We consider 80% participation in testing in both panels.

This illustrates how daily testing when symptom prevalence is 50% or greater, and testing every third day, when symptom prevalence is greater than 75%, are predicted to be more effective than weekly RT-PCR.

Impact of timing of olfactory dysfunction onset

Although olfactory dysfunction is an early symptom of COVID-19 [13–17, 19], there are limited data on the exact timing of symptom onset and its variability between individuals. Given this uncertainty, we performed additional analyses on how olfactory screening would be affected by the timing of symptom onset (Fig. 2). Assuming 80% participation in testing, we considered the central estimates of 75% symptom prevalence and seven days of symptom duration, and varied the timing of symptom onset from coincident with viral loads detectable by RT-PCR to three days after.

We observed that daily, or every three days, olfactory testing was sufficient to keep viral infections from developing into an outbreak, provided that olfactory dysfunction typically occurs within two days of positivity by RT-PCR (Fig. 2). However, when symptom onset was three days after detectable viral loads, epidemic growth was poorly controlled with testing every three days, but could be controlled with daily testing (Figs. 2A and S2A). Weekly testing was largely ineffective when symptom onset was later than coincident with viral loads reaching detectable levels (Fig. S2B).

Impact of olfactory dysfunction duration

Additional analyses argue that olfactory dysfunction screening could be an effective COVID-19 control mechanism even if the duration of olfactory dysfunction is shorter. For these analyses, we considered the case of 80% participation, 75% symptom prevalence, symptom onset one day after viral loads detectable by RT-PCR, and varied the symptom duration from one, three, five, or seven days.

We observed that testing every third day for olfaction controlled epidemic growth when the duration of olfactory dysfunction was three to seven days (Fig. 3). Even if olfactory dysfunction lasted only one

medRxiv preprint doi: https://doi.org/10.1101/2020.11.30.20241174; this version posted December 2, 2020. The copyright holder for this preprint (which was not certified by peer review) is the author/funder, who has granted medRxiv a license to display the preprint in perpetuity. It is made available under a CC-BY-NC-ND 4.0 International license .

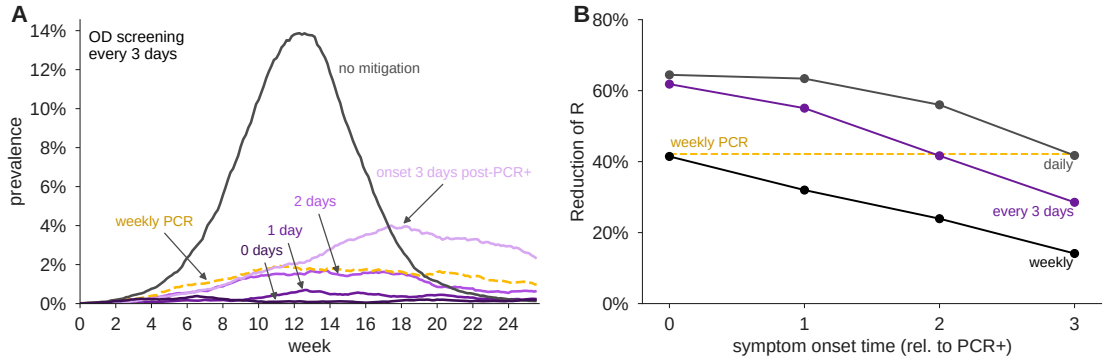

Figure 2: **Impact of the timing of olfactory dysfunction onset on its effectiveness to limit viral spread.** (A) Examples of viral spread in fully-mixed community of 20,000 individuals performing olfactory dysfunction (OD) screening every three days. olfactory dysfunction is modeled to be present in 75% of infected individuals, and to last 7 days. Timing of olfactory dysfunction is varied from coincident with viral levels reaching ∼1000 virions/ml (0 days, darkest purple), one day later (1 day, dark purple), 2 days later (2 days, medium purple), and 3 days later (3 days, light purple). No mitigation is shown as black line. For comparison, weekly RT-PCR testing with a one-day turnaround is shown (yellow). (B) Reduction of reproductive number R with different testing regimens showing the impact of timing of symptom onset with weekly (black line), every three days (purple line), or daily (gray line), testing for olfactory dysfunction. Weekly RT-PCR testing is shown for comparison (yellow dashed line). We consider 80% participation in testing in both panels.

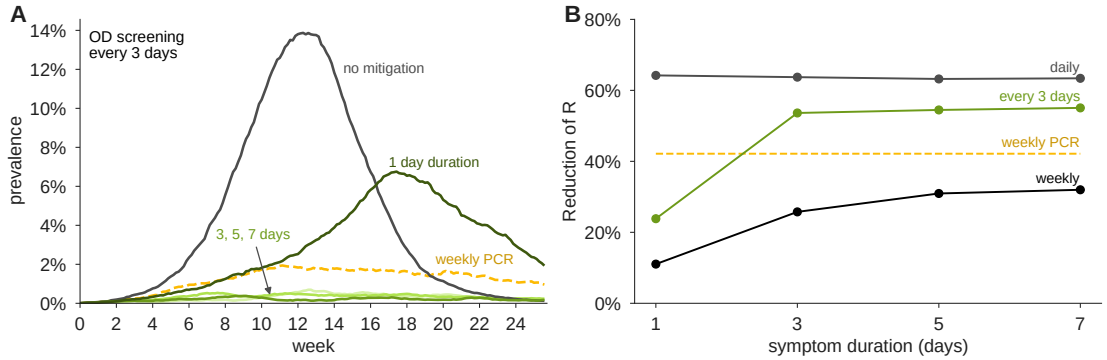

Figure 3: **Impact of duration of olfactory dysfunction on its effectiveness to limit viral spread.** (A) Examples of viral spread in fully-mixed community of 20,000 individuals performing olfactory dysfunction (OD) screening every three days. Olfactory dysfunction is modeled to be present in 75% of infected individuals, and to begin when viral levels reach ∼1000 virions/ml. Duration of olfactory dysfunction is varied from 7 days (lightest green), 5 days (light green), 3 days (green), to 1 day (dark green). No mitigation is shown as black line. For comparison, weekly RT-PCR testing with a one-day turnaround is shown. (B) Reduction of reproductive number R with different testing regimens showing the impact of olfactory dysfunction duration with weekly (black line), every three days (green line), or daily (gray line), testing for olfactory dysfunction. Weekly RT-PCR testing is shown for comparison (yellow dashed line). We consider 80% participation in testing in both panels.

medRxiv preprint doi: https://doi.org/10.1101/2020.11.30.20241174; this version posted December 2, 2020. The copyright holder for this preprint (which was not certified by peer review) is the author/funder, who has granted medRxiv a license to display the preprint in perpetuity. It is made available under a CC-BY-NC-ND 4.0 International license .

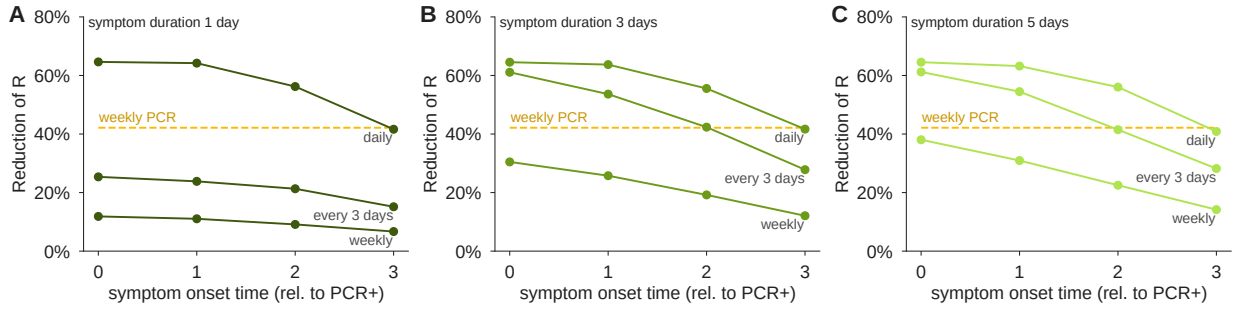

Figure 4: **Impact of the timing of onset and duration of olfactory dysfunction on its effectiveness to limit viral spread.** Reductions of the reproductive number R by testing daily, every third day, or weekly for olfaction dysfunction are shown for olfactory dysfunction lasting (A) one day, (B) three days, and (C) five days, for varying symptom onset times, relative to when viral levels reach $\sim$1000 virions/ml. We consider 80% participation in testing and 75% prevalence of olfactory dysfunction in all panels.

day—unlikely based on current observations—daily testing would nevertheless allow effective control. Weekly testing for olfaction was insufficient to maintain viral control unless olfactory dysfunction persisted for 7 days with onset coincident with detectable virus by RT-PCR (Figs. 3B, S3B, and S4L). To investigate interactions between onset timing and duration, we systematically modeled combinations of each, finding that testing for olfactory dysfunction every three days was effective, as assessed either by reductions in R (Fig. 4) or by viral containment in community simulations (Fig. S4), provided that olfactory dysfunction lasted at least three days, and symptom onset was within 2 days of viral loads detectable by RT-PCR. Importantly, daily olfactory testing was sufficient to control viral spread even when the olfactory dysfunction onset was three days after detectable viral levels and lasted only for a single day (Fig. S4A).

These analyses demonstrate that screening for olfactory dysfunction can be an effective control mechanism, even if average symptom duration is short, and symptom onset occurs within three days of detectable viral loads. More frequent testing for olfaction is required for effective control when the duration of olfactory dysfunction is short, and/or symptom onset is later in viral infection.

Screening for olfactory dysfunction to mitigate an outbreak.

To investigate whether olfactory screening could be effective at controlling an ongoing outbreak, we simulated epidemics in the fully-mixed SEIR model, such that a screening regimen began only when prevalence reached 2% of the population. We used the central estimates of 75% olfactory dysfunction prevalence, symptom onset one day after detectable viral levels, and a symptom duration of 7 days. We observed that screening daily or every third day, with 80% participation, was sufficient to bring the outbreak under control (Fig. 5), and under these conditions, would be more effective than weekly RT-PCR.

Olfactory dysfunction screening regimens are cost-effective

To estimate the costs of modeled interventions, in each simulation we tracked the number of required olfactory dysfunction tests and follow up RT-PCR assays over a 120-day simulation (Table 1). In the repeated testing cases, we assumed individuals with COVID-19-independent olfactory dysfunction would not be tested by RT-PCR, and therefore the estimated costs of RT-PCR are minimum estimates. We found that a mitigation strategy based on weekly RT-PCR assays with 80% participation would reduce R by 42% but

medRxiv preprint doi: https://doi.org/10.1101/2020.11.30.20241174; this version posted December 2, 2020. The copyright holder for this preprint (which was not certified by peer review) is the author/funder, who has granted medRxiv a license to display the preprint in perpetuity. It is made available under a CC-BY-NC-ND 4.0 International license .

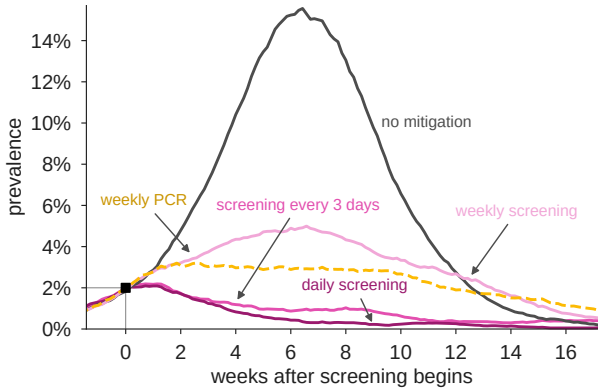

Figure 5: **Impact of olfactory dysfunction screening on an ongoing viral outbreak** Examples of the impact of screening programs based on olfactory dysfunction on controlling an ongoing outbreak. Viral spread in fully-mixed community of 20,000 individuals was allowed to proceed until prevalence reached 2%, at which point olfactory dysfunction (OD) screening was initiated either daily (dark red), every three days (red), or weekly (pink). For comparison, weekly RT-PCR testing with a one-day turnaround is shown (dashed yellow line). Olfactory dysfunction is modeled to be present in 75% of infected individuals, last 7 days, and to begin one day after viral levels reach ∼1000 virions/ml. We consider 80% participation in testing. Scenario without mitigation is shown for comparison (black).

screening regimen	OD tests	PCR tests	cost (millions)	reduction in R	cost effectiveness
OD daily	1,899,109	233	\$0.95	63.4%	66
OD every 3 days	631,549	296	\$0.32	55.1%	171
OD weekly	267,745	948	\$0.15	40.0%	209
PCR every 3 days	–	637,229	\$12.74	68.4%	5.4
PCR weekly	–	265,496	\$5.31	42.1%	8.0

Table 1: **Cost effectiveness of screening programs.** Numbers of olfactory dysfunction (OD) tests and PCR tests ordered are translated to total costs for a 120 day testing program at a rate of \$0.50 per OD test and \$20 per PCR test in simulations of a population of 20,000 individuals with $R_0 = 1.6$, Cost effectiveness is calculated as the percentage reduction in R per million dollars. Individuals positive for olfactory dysfunction received a confirmatory PCR test. Olfactory dysfunction is modeled to be present in 75% of infected individuals, last 7 days, and to begin one day after viral loads reach 1000 virions/ml. We consider 80% participation in testing of either type.

cost \$5.3 million in tests, even at the low rate of \$20 per RT-PCR test (\$100 is more typical). In contrast, mitigation based on olfactory screening every three days with follow-up RT-PCR would cost \$320,000 in tests, assuming \$0.50 per olfactory test, and reduce R by 55% (Table 1). Cost estimates do not include costs of staffing, PPE, or sample collection and transport which may be required for testing via RT-PCR.

Olfactory dysfunction as a point of entry screening tool

Due to the immediate results of currently available olfactory dysfunction tests, we also examined the conditions under which they would be useful as point-of-entry screening tools, analogous to screening of airline passengers or individuals entering a social event with rapid antigen tests. We observed that screening for olfactory dysfunction removed same-day infectiousness in proportion to the fraction of individuals showing that symptom, and was more effective the earlier symptom onset occurred (Fig. S5A). Symptom screening is ∼80% effective when 90% of the infected individuals show the symptom (Fig. S5A). Notably, even with only 50% of infected individuals showing olfactory dysfunction over 40% of infectiousness was removed

medRxiv preprint doi: https://doi.org/10.1101/2020.11.30.20241174; this version posted December 2, 2020. The copyright holder for this preprint (which was not certified by peer review) is the author/funder, who has granted medRxiv a license to display the preprint in perpetuity. It is made available under a CC-BY-NC-ND 4.0 International license .

provided symptom onset occurred no later than one day after sufficient viral load to be detected by RT-PCR testing (Fig. S5A). In contrast, a symptom similar to fever, which is short lived and seen in a small number of infected individuals [5–7], maximally only removes less than 20% of infectiousness (Fig. S5A).

One limitation of using olfaction dysfunction as a single step screen for COVID-19 is the prevalence of non-COVID-19 related olfactory dysfunction, estimated at 3-5% of the population [29–31]. Thus, in screening a population with 1% COVID-19 prevalence, olfactory dysfunction would have low positive predictive value, with 67-80% of olfactory dysfunction due to non-COVID-19 causes. However, a screening regimen where individuals who failed an olfaction test were given a follow-up rapid antigen test was cost effective ($\sim$1.00$/person), reduced false positive that were inappropriately denied entry compared to either test alone, would have rapid turnaround times, and removed greater than 70% of infectiousness when symptom prevalence was 75% or greater (Fig. S5B,C).

Discussion

An important contribution of this modeling is to demonstrate that monitoring of olfactory dysfunction could be effective at controlling the spread of SARS-CoV-2. Our analysis, and data in the literature, argue that olfactory dysfunction during COVID-19 meets all the necessary criteria of prevalence and specificity, timing, and duration for being effective in pandemic control. First, our modeling showed that the estimated 75% prevalence of olfactory dysfunction among those with and without other overt COVID-19 symptoms [9–11] was sufficiently high to have a substantial impact in screening regimens (Fig. 1). Second, we showed that screening would be effective even if anosmia onset is 3 days after detectable levels of virus by RT-PCR, with increasing predicted effectiveness with earlier onset times (Fig. 2). To date, there have been few prospective studies of loss of smell in COVID-19 patients, but existing evidence indicates an earlier onset of anosmia than overt symptom like fever and headache [13–16, 19]. Third, our analysis suggests the even if the duration of olfactory dysfunction is as short as one day (the exact duration and its variability in infected individuals with no other overt symptoms is unknown), frequent monitoring for olfaction can still be effective for epidemic control (Fig. 3). Our simulations suggest effective epidemic mitigation can be achieved under all conditions with daily testing; with longer durations and earlier symptom onset, epidemics can be controlled with testing every three days.

Olfactory screening is inexpensive and scalable, two critical factors for large population-scale testing. Because olfaction tests are inexpensive (we estimate $0.50/test) and uncomplicated, frequent repeated tests can feasibly be carried out by a large fraction of the population. For comparison, to test 50 million people/day (or the entire US population weekly) PCR tests costing $50 each would cost $2.5 billion per day, $10 antigen tests would still cost $500 million per day, while an olfactory test would cost $25 million per day— between 10$\times$ and 100$\times$ less. Moreover, since olfaction can be self-tested, there is no need for the logistics of sample collection and transport, which can further reduce costs.

A potential advantage of olfactory screening is its ability to be scaled. Paper-based olfactory dysfunction tests can be printed on industrial printers and a single commercial printing facility can produce over 50 million tests daily (D.T., communication). Simple olfaction tests linked to a mobile phone app have already been developed, are FDA registered, and are under consideration for Emergency Use Authorization (EUA) by the U.S. FDA for COVID-19 applications, as of November 2020. In contrast, current PCR testing maximum capacity is approximately 2.1 million tests/day.[2] Moreover, instant olfactory symptom reporting via a

[2]COVID Tracking Project, as of Nov. 28, 2020; https://covidtracking.com/data.

medRxiv preprint doi: https://doi.org/10.1101/2020.11.30.20241174; this version posted December 2, 2020. The copyright holder for this preprint (which was not certified by peer review) is the author/funder, who has granted medRxiv a license to display the preprint in perpetuity. It is made available under a CC-BY-NC-ND 4.0 International license .

testing app could provide centralized surveillance and early warning of new outbreaks [16].

Our study is subject to a number of limitations. First, our modeling assumed that olfaction tests would not only correctly identify those with olfactory dysfunction, but would remain sensitive during regular use. Repeated use of the same test could lead to adaptation or memorization, decreasing test sensitivity. Second, we assumed that no individual would intentionally fail a test–an issue only averted with reflex molecular testing. Finally, we assumed that olfactory dysfunction revealed by a test would lead to isolation, but this assumption is unlikely to be valid for essential workers, or those uninterested in adherence to an isolation protocol. These limitations highlight the need to develop, deploy in trial situations, and refine tests for olfaction that can be mass produced at low cost and self-administered.

There are three additional points to consider in implementing olfactory screening for COVID-19 control. First, when a new community is subject to olfactory screening, there will be an initial surge of individuals identified with olfactory dysfunction both due to undetected COVID-19 infections, and COVID-19-independent olfactory dysfunction (anosmia and hyposmia). This will require the ability to handle a reflexive surge in molecular testing during the initial phase. However, even in the absence of follow-up molecular testing, unnecessary quarantines of those without COVID-19 (false positives) should be weighed against blanket non-pharmaceutical interventions such as lockdowns and curfews. A second issue is that increased anosmia in older adults [29, 30] will mean that olfactory screening will be most effective with younger adults, including college students and school children. Finally, a critical public health issue inherent to any COVID-19 monitoring/surveillance mechanism is that no testing strategy identifies and isolates all the COVID-19 infected individuals, both from false negatives, and from new import of infections into a community. Therefore, any COVID-19 screening regimen must complement and not replace existing viral mitigation mechanisms such as mask wearing and social distancing.

References

[1] Melissa M Arons, Kelly M Hatfield, Sujan C Reddy, Anne Kimball, Allison James, Jesica R Jacobs, Joanne Taylor, Kevin Spicer, Ana C Bardossy, Lisa P Oakley, et al. Presymptomatic SARS-CoV-2 infections and transmission in a skilled nursing facility. *New England Journal of Medicine*, 2020.

[2] Desmond Sutton, Karin Fuchs, Mary D'alton, and Dena Goffman. Universal screening for SARS-CoV-2 in women admitted for delivery. *New England Journal of Medicine*, 2020.

[3] Daniel P Oran and Eric J Topol. Prevalence of asymptomatic SARS-CoV-2 infection: A narrative review. *Annals of Internal Medicine*, 2020.

[4] Philip Dollard, Isabel Griffin, Andre Berro, Nicole J Cohen, Kimberly Singler, Yoni Haber, Chris de la Motte Hurst, Amber Stolp, Sukhshant Atti, Leslie Hausman, et al. Risk assessment and management of covid-19 among travelers arriving at designated us airports, january 17–september 13, 2020. *Morbidity and Mortality Weekly Report*, 69(45):1681, 2020.

[5] Michel Bielecki, Giovanni Andrea Gerardo Crameri, Patricia Schlagenhauf, Thomas Werner Buehrer, and Jeremy Werner Deuel. Body temperature screening to identify SARS-CoV-2 infected young adult travellers is ineffective. *Travel Medicine and Infectious Disease*, 2020.

[6] James L Rudolph, Christopher W Halladay, Malisa Barber, Kevin McCongehy, Vince Mor, Aman Nanda, and Stefan Gravenstein. Temperature in nursing home residents systematically tested for SARS-CoV-2. *Journal of the American Medical Directors Association*, 2020.

medRxiv preprint doi: https://doi.org/10.1101/2020.11.30.20241174; this version posted December 2, 2020. The copyright holder for this preprint (which was not certified by peer review) is the author/funder, who has granted medRxiv a license to display the preprint in perpetuity. It is made available under a CC-BY-NC-ND 4.0 International license .

[7] Gary M Vilke, Jesse J Brennan, Alexandrea O Cronin, and Edward M Castillo. Clinical features of patients with COVID-19: is temperature screening useful? *The Journal of Emergency Medicine*, 2020.

[8] AA Chughtai, Q Wang, TC Dung, and CR Macintyre. The presence of fever in adults with influenza and other viral respiratory infections. *Epidemiology & Infection*, 145(1):148–155, 2017.

[9] Akosua Adom Agyeman, Ken Lee Chin, Cornelia B Landersdorfer, Danny Liew, and Richard Ofori-Asenso. Smell and taste dysfunction in patients with COVID-19: A systematic review and meta-analysis. In *Mayo Clinic Proceedings*. Elsevier, 2020.

[10] Khang Wen Pang, Jeremy Chee, Somasundaram Subramaniam, and Chew Lip Ng. Frequency and clinical utility of olfactory dysfunction in COVID-19: a systematic review and meta-analysis. *Current allergy and asthma reports*, 20(12):1–17, 2020.

[11] Anindya S Bhattacharjee, Samir V Joshi, Shilpa Naik, Shashikala Sangle, and Nixon M Abraham. Quantitative assessment of olfactory dysfunction accurately detects asymptomatic COVID-19 carriers. *EClinicalMedicine*, page 100575, 2020.

[12] Daniel C Payne, Sarah E Smith-Jeffcoat, Gosia Nowak, Uzo Chukwuma, Jesse R Geibe, Robert J Hawkins, Jeffrey A Johnson, Natalie J Thornburg, Jarad Schiffer, Zachary Weiner, et al. SARS-CoV-2 infections and serologic responses from a sample of us navy service members—uss theodore roosevelt, april 2020. *Morbidity and Mortality Weekly Report*, 69(23):714, 2020.

[13] Rafal Butowt and Christopher S von Bartheld. Anosmia in COVID-19: Underlying mechanisms and assessment of an olfactory route to brain infection. *The Neuroscientist*, page 1073858420956905, 2020.

[14] Yonghyun Lee, Pokkee Min, Seonggu Lee, and Shin-Woo Kim. Prevalence and duration of acute loss of smell or taste in COVID-19 patients. *Journal of Korean medical science*, 35(18), 2020.

[15] Shima T Moein, Seyed MR Hashemian, Babak Mansourafshar, Ali Khorram-Tousi, Payam Tabarsi, and Richard L Doty. Smell dysfunction: a biomarker for COVID-19. In *International forum of allergy & rhinology*. Wiley Online Library, 2020.

[16] Denis Pierron, Veronica Pereda-Loth, Marylou Mantel, Maëlle Moranges, Emmanuelle Bignon, Omar Alva, Julie Kabous, Margit Heiske, Jody Pacalon, Renaud David, et al. Smell and taste changes are early indicators of the covid-19 pandemic and political decision effectiveness. *Nature communications*, 11(1):1–8, 2020.

[17] Marlene M Speth, Thirza Singer-Cornelius, Michael Oberle, Isabelle Gengler, Steffi J Brockmeier, and Ahmad R Sedaghat. Mood, anxiety and olfactory dysfunction in COVID-19: evidence of central nervous system involvement? *The Laryngoscope*, 130(11):2520–2525, 2020.

[18] Luigi Angelo Vaira, Giovanna Deiana, Alessandro Giuseppe Fois, Pietro Pirina, Giordano Madeddu, Andrea De Vito, Sergio Babudieri, Marzia Petrocelli, Antonello Serra, Francesco Bussu, et al. Objective evaluation of anosmia and ageusia in COVID-19 patients: Single-center experience on 72 cases. *Head & neck*, 42(6):1252–1258, 2020.

medRxiv preprint doi: https://doi.org/10.1101/2020.11.30.20241174; this version posted December 2, 2020. The copyright holder for this preprint (which was not certified by peer review) is the author/funder, who has granted medRxiv a license to display the preprint in perpetuity. It is made available under a CC-BY-NC-ND 4.0 International license .

[19] Tyler Wagner, FNU Shweta, Karthik Murugadoss, Samir Awasthi, AJ Venkatakrishnan, Sairam Bade, Arjun Puranik, Martin Kang, Brian W Pickering, John C O'Horo, et al. Augmented curation of clinical notes from a massive ehr system reveals symptoms of impending COVID-19 diagnosis. *Elife*, 9:e58227, 2020.

[20] Alberto Paderno, Davide Mattavelli, Vittorio Rampinelli, Alberto Grammatica, Elena Raffetti, Michele Tomasoni, Tommaso Gualtieri, Stefano Taboni, Silvia Zorzi, Francesca Del Bon, et al. Olfactory and gustatory outcomes in COVID-19: A prospective evaluation in nonhospitalized subjects. *Otolaryngology–Head and Neck Surgery*, 2020.

[21] Jerome R Lechien, Carlos M Chiesa-Estomba, Daniele R De Siati, Mihaela Horoi, Serge D Le Bon, Alexandra Rodriguez, Didier Dequanter, Serge Blecic, Fahd El Afia, Lea Distinguin, et al. Olfactory and gustatory dysfunctions as a clinical presentation of mild-to-moderate forms of the coronavirus disease (COVID-19): a multicenter european study. *European Archives of Oto-Rhino-Laryngology*, pages 1–11, 2020.

[22] Daniel B Larremore, Bryan Wilder, Evan Lester, Soraya Shehata, James M Burke, James A Hay, Milind Tambe, Michael J Mina, and Roy Parker. Test sensitivity is secondary to frequency and turnaround time for COVID-19 surveillance. *MedRxiv*, 2020.

[23] Michael J Mina, Roy Parker, and Daniel B Larremore. Rethinking COVID-19 test sensitivity—a strategy for containment. *New England Journal of Medicine*, 2020.

[24] A David Paltiel, Amy Zheng, and Rochelle P Walensky. Assessment of SARS-CoV-2 screening strategies to permit the safe reopening of college campuses in the united states. *JAMA network open*, 3(7):e2016818–e2016818, 2020.

[25] Stephen Kissler, Nishant Kishore, Malavika Prabhu, Dena Goffman, Yaakov Beilin, Ruth Landau, Cynthia Gyamfi-Bannerman, Brian Bateman, Daniel Katz, Jonathan Gal, Angela Bianco, Joanne Stone, Daniel Larremore, Caroline Buckee, and Yonatan Grad. Reductions in commuting mobility correlate with geographic differences in SARS-CoV-2 prevalence in New York City. *Nature Communications*, 11(1):1–6, 2020.

[26] Muge Cevik, Matthew Tate, Oliver Lloyd, Alberto Enrico Maraolo, Jenna Schafers, and Antonia Ho. SARS-CoV-2, sars-cov-1 and mers-cov viral load dynamics, duration of viral shedding and infectiousness: a living systematic review and meta-analysis. *medRxiv*, 2020.

[27] Amber M Smith and Alan S Perelson. Influenza A virus infection kinetics: quantitative data and models. *Wiley Interdisciplinary Reviews: Systems Biology and Medicine*, 3(4):429–445, 2011.

[28] Mathilde Richard, Adinda Kok, Dennis de Meulder, Theo M Bestebroer, Mart M Lamers, Nisreen MA Okba, Martje Fentener van Vlissingen, Barry Rockx, Bart L Haagmans, Marion PG Koopmans, et al. SARS-CoV-2 is transmitted via contact and via the air between ferrets. *bioRxiv*, 2020.

[29] Sanne Boesveldt, Elbrich M Postma, Duncan Boak, Antje Welge-Luessen, Veronika Schöpf, Joel D Mainland, Jeffrey Martens, John Ngai, and Valerie B Duffy. Anosmia—a clinical review. *Chemical senses*, 42(7):513–523, 2017.

medRxiv preprint doi: https://doi.org/10.1101/2020.11.30.20241174; this version posted December 2, 2020. The copyright holder for this preprint (which was not certified by peer review) is the author/funder, who has granted medRxiv a license to display the preprint in perpetuity. It is made available under a CC-BY-NC-ND 4.0 International license .

[30] Andreas Hinz, Tobias Luck, Steffi G Riedel-Heller, Philipp Y Herzberg, Claudia Rolffs, Kerstin Wirkner, and Christoph Engel. Olfactory dysfunction: properties of the sniffin'sticks screening 12 test and associations with quality of life. *European Archives of Oto-Rhino-Laryngology*, 276(2):389–395, 2019.

[31] Jingpu Yang and Jayant M Pinto. The epidemiology of olfactory disorders. *Current otorhinolaryngology reports*, 4(2):130–141, 2016.

[32] Stephen M Kissler, Joseph R Fauver, Christina Mack, Caroline Tai, Kristin Y Shiue, Chaney Kalinich, Sarah Jednak, Isabel Ott, Chantal Vogels, Jay Wohlgemuth, et al. Viral dynamics of SARS-CoV-2 infection and the predictive value of repeat testing. *medRxiv*, 2020.

[33] Kendra Quicke, Emily Gallichote, Nicole Sexton, Michael Young, Ashley Janich, Gregory Gahm, Elizabeth J Carlton, Nicole Ehrhart, and Gregory D Ebel. Longitudinal surveillance for SARS-CoV-2 RNA among asymptomatic staff in five colorado skilled nursing facilities: Epidemiologic, virologic and sequence analysis. *medRxiv*, 2020.

[34] Roman Wölfel, Victor M Corman, Wolfgang Guggemos, Michael Seilmaier, Sabine Zange, Marcel A Müller, Daniela Niemeyer, Terry C Jones, Patrick Vollmar, Camilla Rothe, et al. Virological assessment of hospitalized patients with COVID-2019. *Nature*, 581(7809):465–469, 2020.

[35] Bernard La Scola, Marion Le Bideau, Julien Andreani, Van Thuan Hoang, Clio Grimaldier, Philippe Colson, Philippe Gautret, and Didier Raoult. Viral RNA load as determined by cell culture as a management tool for discharge of SARS-CoV-2 patients from infectious disease wards. *European Journal of Clinical Microbiology & Infectious Diseases*, 39(6):1059, 2020.

Acknowledgements

The authors thank Yonatan Grad for valuable feedback. This work was supported by the Howard Hughes Medical Institute (Roy Parker).

Author Contributions

D.B.L., D.T., and R.P. conceived and designed the study. D.B.L. performed the computational modeling. D.B.L., D.T., and R.P. wrote the manuscript.

Data Availability

All data needed to evaluate the conclusions in the paper are present in the paper and/or the Supplementary Materials, and open-source code is available at https://github.com/LarremoreLab/covid_olfactory_dysfunction.

Competing Interests

D.B.L. is a member of the scientific advisory board of Darwin BioSciences. D.T. is a founder of an olfactory test company u-Smell-it LLC and has related pending patents.

medRxiv preprint doi: https://doi.org/10.1101/2020.11.30.20241174; this version posted December 2, 2020. The copyright holder for this preprint (which was not certified by peer review) is the author/funder, who has granted medRxiv a license to display the preprint in perpetuity. It is made available under a CC-BY-NC-ND 4.0 International license .

Materials and Methods

Individual infection model

Each individual infection consists of four key elements: (1) a viral load trajectory which charts the measurable concentration of virus over the course of infection, (2) the presence of symptoms so noticeable that they cause a change in behavior, i.e. symptom-driven self-isolation, (3) the presence of symptoms identifiable by a screening test, such as anosmia or low fever, and (4) an infectiousness trajectory, which is related to both viral load and behavior. Each of these components is described in detail below.

When a positive screening test—virological or symptom-based—provides a positive test result during the individual's infectious window, prior to any self-isolation, that person is assumed to isolate for the remainder of the infection. Thus, depending on the individual's viral load, infectiousness, timing of possible test results, and timing of possible self-isolation, a screening test may or may not cause an individual's isolation and concomitant decrease in circulating infectiousness.

Viral Load Trajectories. Viral loads were drawn from a simple, previously published viral kinetics model which captures four key aspects of a SARS-CoV-2 infection [22]: (a) a variable latent period, (b) a rapid proliferation phase from the lower limit of PCR detectability to a peak viral load, (c) a slower clearance phase, and (d) prolonged clearance for symptomatic infections vs asymptomatic infections. These dynamics were based on a growing body of literature that includes longitudinal repeated PCR sampling of symptomatic and asymptomatic individuals, in both prospective and non-prospective contexts. The detailed studies on which the viral load was based were previously reviewed in [22], but have since been further supported through a prospective longitudinal study [32] which further refined the proliferation phase and differential clearance rates based on symptoms.

To summarize the model of Ref. [22], with slight modifications to reflect knowledge gained from Ref. [32], $\log_{10}$ viral loads were approximated by a continuous piecewise linear "hinge" function, specified uniquely with three control points: $(t_0, 3)$, $(t_{\text{peak}}, V_{\text{peak}})$,$(t_f, 6)$. The first point represents the time at which an individual's viral load first crosses 10^3, and becomes detectable via PCR, with $t_{\text{PRCR}} \sim \text{unif}[2.5, 3.5]$, measured in days since exposure. The second point represents the peak viral load. Peak height was drawn $V_{\text{peak}} \sim \text{unif}[7, 11]$, and peak timing was drawn with respect to the start of the proliferation phase, $t_{\text{peak}} - t_{\text{PCR}} \sim 0.5 + \text{gamma}(2.5)$ with a maximum of 4. The third point represents the time at which an individual's viral load crosses beneath the 10^6 threshold, at which point viral loads no longer cause active cultures in laboratory experiments [26, 33–35]. For asymptomatic infections, this point was drawn with respect to peak timing, $t_f - t_{\text{peak}} \sim \text{unif}[4, 8]$. For overtly symptomatic infections, a symptom onset time was first drawn with respect to peak timing, $t_{\text{symptoms}} - t_{\text{peak}} \sim \text{unif}[0, 2]$, and then the third control point was drawn with respect to symptom onset, $t_f - t_{\text{symptoms}} \sim \text{unif}[4, 8]$. Thus, overtly symptomatic trajectories are systematically longer, in both duration of infectiousness and duration of viral shedding [32]. In simulations, each viral load's parameters were drawn independently of others, and the continuous function described here was evaluated at 21 integer time points, representing a three week span of viral load values.

Overt symptoms causing self-isolation. For individuals with overtly symptomatic infections (see description of Viral Load Trajectories), symptom onset at t_{symptoms} caused self-isolation on the following day. Overt symptoms were assumed to be present in 35% of individuals, and were assumed to be present independently of olfactory dysfunction and low-grade fever, which are considered separately because they typically do not lead to behavior change.

medRxiv preprint doi: https://doi.org/10.1101/2020.11.30.20241174; this version posted December 2, 2020. The copyright holder for this preprint (which was not certified by peer review) is the author/funder, who has granted medRxiv a license to display the preprint in perpetuity. It is made available under a CC-BY-NC-ND 4.0 International license .

Symptoms identifiable by screening. Symptoms such as anosmia or low-grade fever were modeled using three variables which controlled the prevalence θ, onset time t_{onset}, and duration d of symptoms. Onset times were chosen relative to detectability by PCR, such that $t_{\text{onset}} = t_{\text{PCR}} + k$, with $k = -2, -1, \ldots, 3$ evaluated in the text. Note that the prevalence parameter θ incorporates both the presence and the detectability of symptoms. As noted above, the prevalence of identifiable symptoms via this mechanism was considered independently of the overt symptoms that lead to self-isolation.

Infectiousness. Infectiousness F was assumed to be directly related to viral load V in that each individual's relative infectiousness was proportional to the $\log_{10}$ of viral load's excess beyond 10^6, i.e. $F \propto \log_{10}(V) - 6$. For individuals in isolation, either following a positive screening test or following the appearance of overt symptoms (at t_{symptoms}), infectiousness was set to zero. In all simulations, the value of the proportionality constant implied by the infectiousness function was chosen to achieve the targeted value of R_0 for that simulation, and confirmed via simulation as described below.

One-shot, Two-shot, and Repeated Screening

For an individual with viral load trajectory V and infectiousness F over the simulated 21 days of infection, proliferation, and clearance, testing was implemented on a specified day or on a schedule, as follows. First, each individual's viral load V was drawn as described above, with 35% of individuals receiving an overtly symptomatic trajectory and 65% receiving an overtly asymptomatic trajectory. Each individual was also assigned screenable symptoms with probability θ, lasting from day t_{onset} through $t_{\text{onset}} + d$, and no screenable symptoms otherwise.

One-shot and two-shot screening. For disease transmission dynamics scenarios, on the day of one-shot screening, each individual was evaluated to determine whether they would receive a positive test result that day (symptom screening) or the next day (virological screening). Thus, the timing of each individual's viral load, symptom status, and infection status were determined by the dynamics of the simulation, described below. For non-dynamic scenarios, a statistical sample of $10,000$ infected individuals were considered such that the timing of the screening test was equiprobable on each day of infection, with symptom screening and virological results returned on the same day and next day, respectively. Anosmia tests were assumed to have a specificity of 0.96.

In two-shot screening scenarios, individuals with positive symptom screening tests were referred to a reflex point-of-care rapid diagnostic test with an assumed limit of detection L. If $V(t) > L$ on that day, they received a positive result and isolated, but otherwise, they received a negative result and were allowed to enter the imagined event. Rapid diagnostic tests were assumed to have a specificity of 0.025. False positives by anosmia test and by rapid diagnostic test were assumed to be statistically independent of each other, such that the specificity of the two-shot screening was 0.001.

Repeated screening. Based on a schedule of testing each person every D days, if an individual happened to be tested by a symptom screening test on a day when their symptoms were present, their positive result would cause them isolate that day, without delay. Similarly, if an individual happened to be tested by a virological test on a day when their viral load exceeded the limit of detection of the test ($V(t) > L$), their positive result would cause them to isolate, but with a one-day delay in virological test results. Each person was deterministically tested exactly every D days, but testing days were drawn uniformly at random such that not all individuals were tested on the same day. Values of D were $1, 3$ or 7. In repeated screening scenarios, anosmia tests were assumed to have a specificity of 1, reflecting a steady-state assumption that individuals would rapidly determine that their olfactory dysfunction was not COVID-19-related.

medRxiv preprint doi: https://doi.org/10.1101/2020.11.30.20241174; this version posted December 2, 2020. The copyright holder for this preprint (which was not certified by peer review) is the author/funder, who has granted medRxiv a license to display the preprint in perpetuity. It is made available under a CC-BY-NC-ND 4.0 International license .

Disease Transmission Model

A fully-mixed model of $N = 20,000$ individuals with all-to-all contact structure, zero initial infections, and a constant $1/N$ per-person probability of becoming infected from an external source was used to simulate SARS-CoV-2 dynamics, based on a typical compartmental framework, as described in Ref. [22] but with modifications for symptom screening. This models tracked discrete individuals who were Susceptible (S), Infected (I), Recovered (R), Isolated (Q), and Self-Isolated (SQ) at each discrete one-day timestep. Upon becoming infected ($S \to I$), a viral load trajectory $V(t)$ was drawn which included a latent period, growth, and decay as described above. For those chosen to have non-overt symptoms, the timing and duration were fixed, according the choice of parameters and the t_{PCR} of the viral load. Thus, each day, an individual's viral load trajectory was used to determine whether their diagnostic test would be positive if administered, as well as their infectiousness to susceptible individuals; The timing, duration, and prevalence of symptoms was used similarly to determine whether a screening test would be positive if administered.

Participation in testing. A fraction of individuals were, in some simulations, selected to refuse testing. Testing refusal—or its complement, participation—was determined at random using a specified refusal rate, at the initialization of each simulation, and was unchanged for the duration of each simulation.

Isolation due to symptom screening or virological testing. On the specified day(s) of testing, each infected person was evaluated to determine whether their viral load ($V(t) > L$ in the case of a virological test) or symptoms (presence/absence for that individual on that day, in the case of a symptom screening test) would cause a positive test result. Positive results caused isolation ($I \to Q$) with no delay or with a one-day delay for symptom screening or virological tests, respectively.

Self-isolation and recovery. 35% of individuals self-isolate on the day of symptom onset, which occurs 0 to 3 days after peak viral load (see above), to mimic overt symptom-driven isolation ($I \to SQ$). Thus, presymptomatic individuals were isolated prior to symptom onset only if they received positive test results. When an individual's viral load dropped below 10^3, that individual recovered ($I, Q, SQ \to R$).

Transmission, Population Structure, and Mixing Patterns. Simulations were initialized with all individuals susceptible, $S = N$. Each individual was initially chosen to either participate in testing or refused testing, as described above, independently with a probability specified per-simulation. Each individual was chosen to be overtly symptomatic independently with probability 0.35. Both participation/refusal and overt symptoms were assumed to be persistent through the simulation, per person. If repeated testing was to be performed, each individual's first test day (e.g. the day of the week that their weekly test would occur) was chosen uniformly at random between 1 and D. Relative infectiousness was scaled up or down to achieve the specified R_0 in the absence of any testing policy, but inclusive of any assumed self-isolation of overt symptomatics.

In each timestep, those individuals who were marked for testing that day were tested. Individuals receiving a positive test result that day, after delay of virological test results, were isolated, $I \to Q$. Overtly symptomatic individuals whose viral load had declined relative to the previous day were self-isolated, $I \to SQ$. Next, each susceptible individual was spontaneously (externally) infected independently with probability $1/N$, $S \to I$. Then, all infected individuals contacted all susceptible individuals, with the probability of transmission based on that day's viral load $V(t)$ for each person infectiousness function described above, $S \to I$.

To conclude each time step, individuals' viral loads and symptoms were advanced to the next time step, with those whose infectious period had completely passed moved to recovery, $I, Q, SQ \to R$.

medRxiv preprint doi: https://doi.org/10.1101/2020.11.30.20241174; this version posted December 2, 2020. The copyright holder for this preprint (which was not certified by peer review) is the author/funder, who has granted medRxiv a license to display the preprint in perpetuity. It is made available under a CC-BY-NC-ND 4.0 International license .

Ongoing screening vs outbreak mitigation scenarios. In ongoing screening scenarios, simulations with $R_0 = 1.6$ and the constant rate of external infection were conducted with screening beginning, as described above, starting on the first timestep. In outbreak mitigation scenarios, simulations were identical except that no screening was performed until disease prevalence in that time step reached 4% of the population (800 individuals).

Calibration to achieve targeted R_0 and estimation of R

As a consistency check, each simulation's R_0 was confirmed to ensure that simulations were properly calibrated to their intended values. Note that to vary R_0, the proportionality constant in the function that maps viral load to infectiousness need only be adjusted up or down. In a typical SEIR model, this would correspond to changing the infectiousness parameter which governs the rate at which I-to-S contacts cause new infections β.

For the fully-mixed model, the value of R_0 was numerically estimated by running single-generation simulations in which a 50 infected individual were placed in a population of $N - 50$ others. The number of secondary infections from those initially infected was recorded and used to directly estimate R_0.

Estimations of R proceeded exactly as estimations of R_0 for both models, except with interventions applied to the the viral loads, symptoms, and therefore the dynamics.

medRxiv preprint doi: https://doi.org/10.1101/2020.11.30.20241174; this version posted December 2, 2020. The copyright holder for this preprint (which was not certified by peer review) is the author/funder, who has granted medRxiv a license to display the preprint in perpetuity. It is made available under a CC-BY-NC-ND 4.0 International license .

Supplemental Figures and Tables

Contents

- Supplementary Figures S1-S5
- Supplementary Text

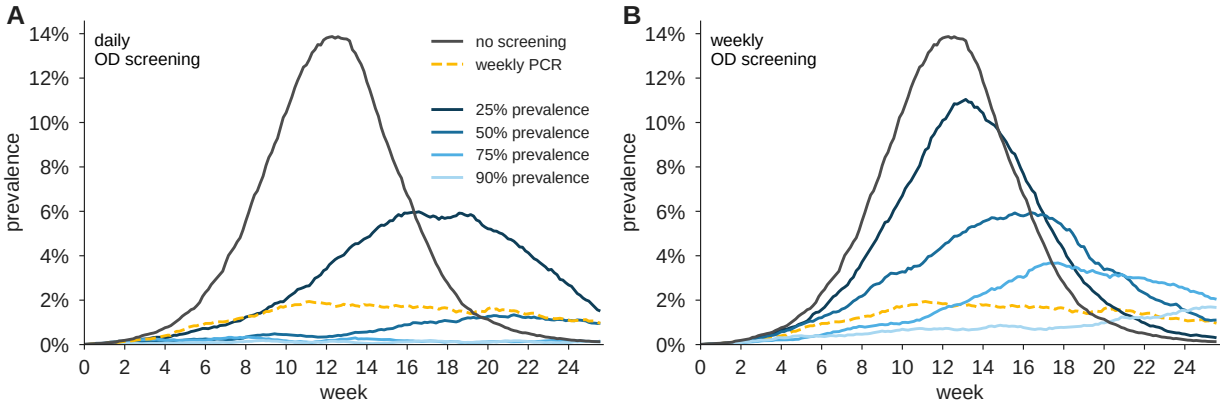

Figure S1: **Impact of olfactory dysfunction prevalence on its effectiveness to limit viral spread.** The figure shows examples of viral spread in fully-mixed community of 20,000 individuals performing olfactory dysfunction (OD) screening daily (A), or weekly (B). No mitigation (black), Prevalence of symptom shown are: 25% (dark blue), 50% (medium blue), 75% (light blue), 90% (lightest blue). For comparison, weekly RT-PCR testing with a one-day turnaround is shown. In this analysis, olfactory dysfunction is modeled to last 7 days, and begin when viral levels reach 1000 virions/ml. We consider 80% participation in testing.

medRxiv preprint doi: https://doi.org/10.1101/2020.11.30.20241174; this version posted December 2, 2020. The copyright holder for this preprint (which was not certified by peer review) is the author/funder, who has granted medRxiv a license to display the preprint in perpetuity. It is made available under a CC-BY-NC-ND 4.0 International license .

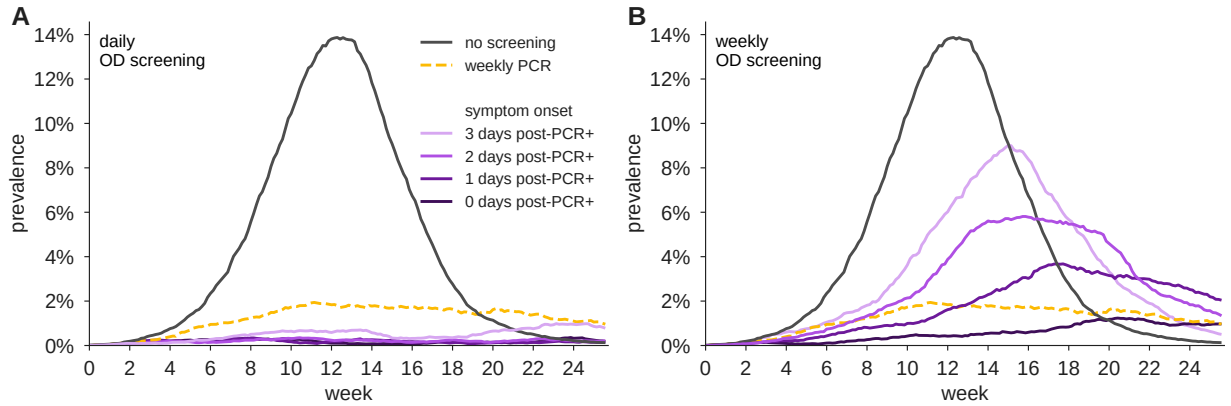

Figure S2: **Impact of the timing of olfactory dysfunction onset on its effectiveness to limit viral spread.** Example of viral spread in fully-mixed community of 20,000 individuals performing olfactory dysfunction (OD) screening daily (A) or weekly (B). olfactory dysfunction is modeled to be present in 75% of infected individuals, and to last 7 days. We consider 80% participation in testing. Timing of olfactory dysfunction is varied from coincident with virions levels reaching 1000 virions/ml (0 days, darkest purple), one day later (1 day, dark purple), 2 days later (2 days, medium purple), and 3 days later (3 days, light purple). No mitigation is shown as black line. For comparison, weekly RT-PCR testing with a one-day turnaround is shown.

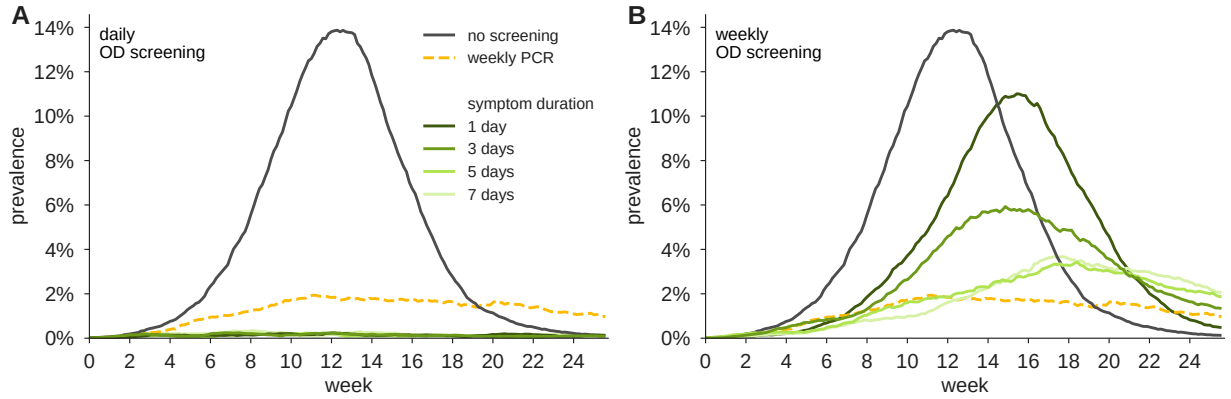

Figure S3: **Impact of duration of olfactory dysfunction on its effectiveness to limit viral spread.** Examples of viral spread in fully-mixed community of 20,000 individuals performing olfactory dysfunction (OD) screening daily (A) or weekly (B). olfactory dysfunction is modeled to be present in 75% of infected individuals, and to begin when virion levels reach 1000 virions/ml. We consider 80% participation in testing. Duration of olfactory dysfunction is varied from 7 days (lightest green), 5 days (light green), 3 days (green), to 1 day (dark green). No mitigation is shown as black line. For comparison, weekly RT-PCR testing with a one-day turnaround is shown.

medRxiv preprint doi: https://doi.org/10.1101/2020.11.30.20241174; this version posted December 2, 2020. The copyright holder for this preprint (which was not certified by peer review) is the author/funder, who has granted medRxiv a license to display the preprint in perpetuity. It is made available under a CC-BY-NC-ND 4.0 International license .

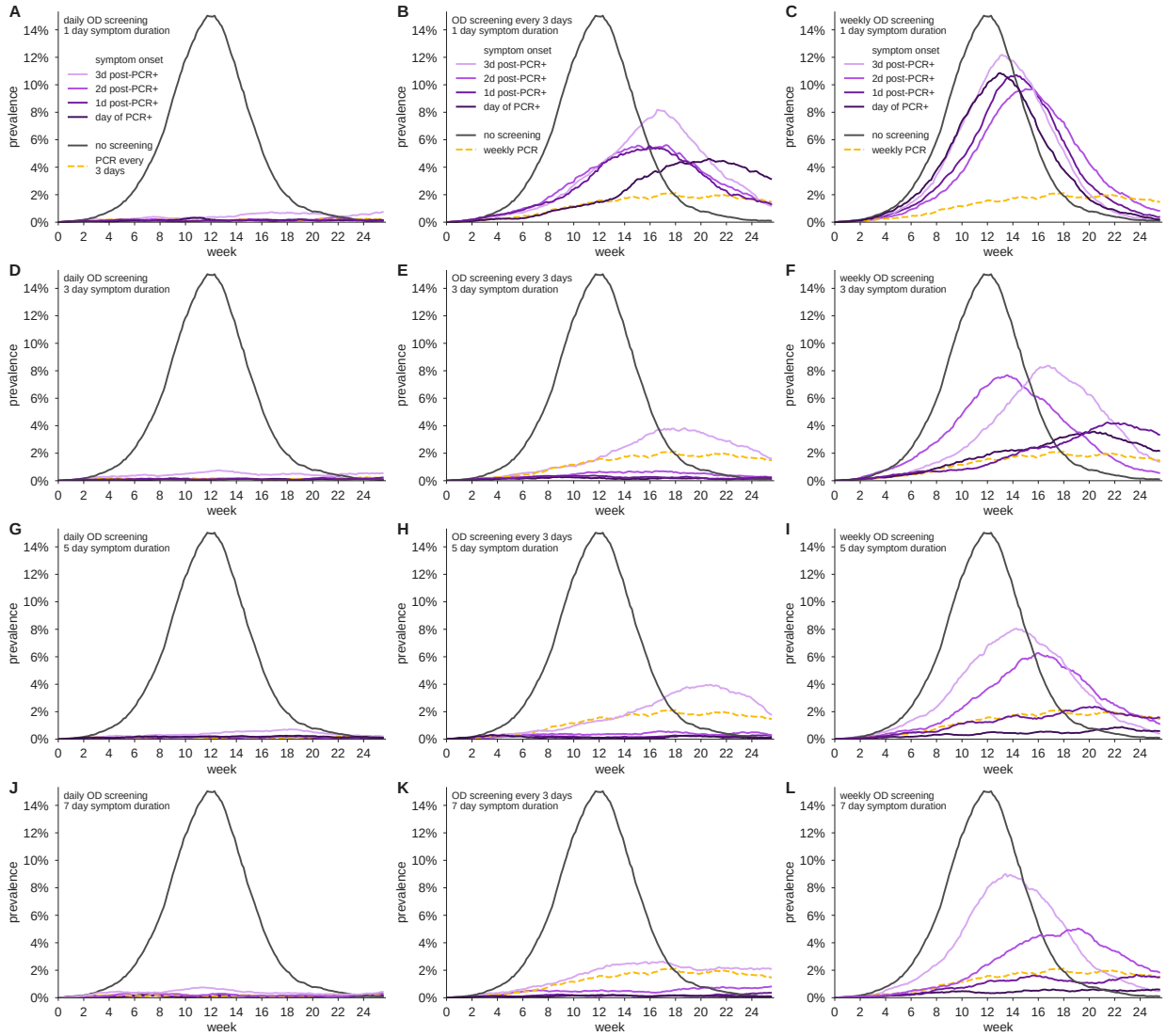

Figure S4: **Impact of varying duration and onset time of olfactory dysfunction on its effectiveness to limit viral spread.** Examples of viral spread in fully-mixed community of 20,000 individuals performing olfactory dysfunction (OD) screening daily for symptoms lasting (A, B, C) one day, (D, E, F) three days, (G, H, I) five days, and (J, K, L) seven days, screening every day (left column), every three days (middle column) and weekly (right column). olfactory dysfunction is modeled to be present in 75% of infected individuals, and to begin after 1, 2, or 3 days from when virion levels reach 1000 virions/ml, indicated by varying shades of purple (see legend). We consider 80% participation in testing. No mitigation is shown as black line. For comparison, RT-PCR testing with a one-day turnaround is shown with testing every three days (left column) or weekly (middle and right columns).

medRxiv preprint doi: https://doi.org/10.1101/2020.11.30.20241174; this version posted December 2, 2020. The copyright holder for this preprint (which was not certified by peer review) is the author/funder, who has granted medRxiv a license to display the preprint in perpetuity. It is made available under a CC-BY-NC-ND 4.0 International license .

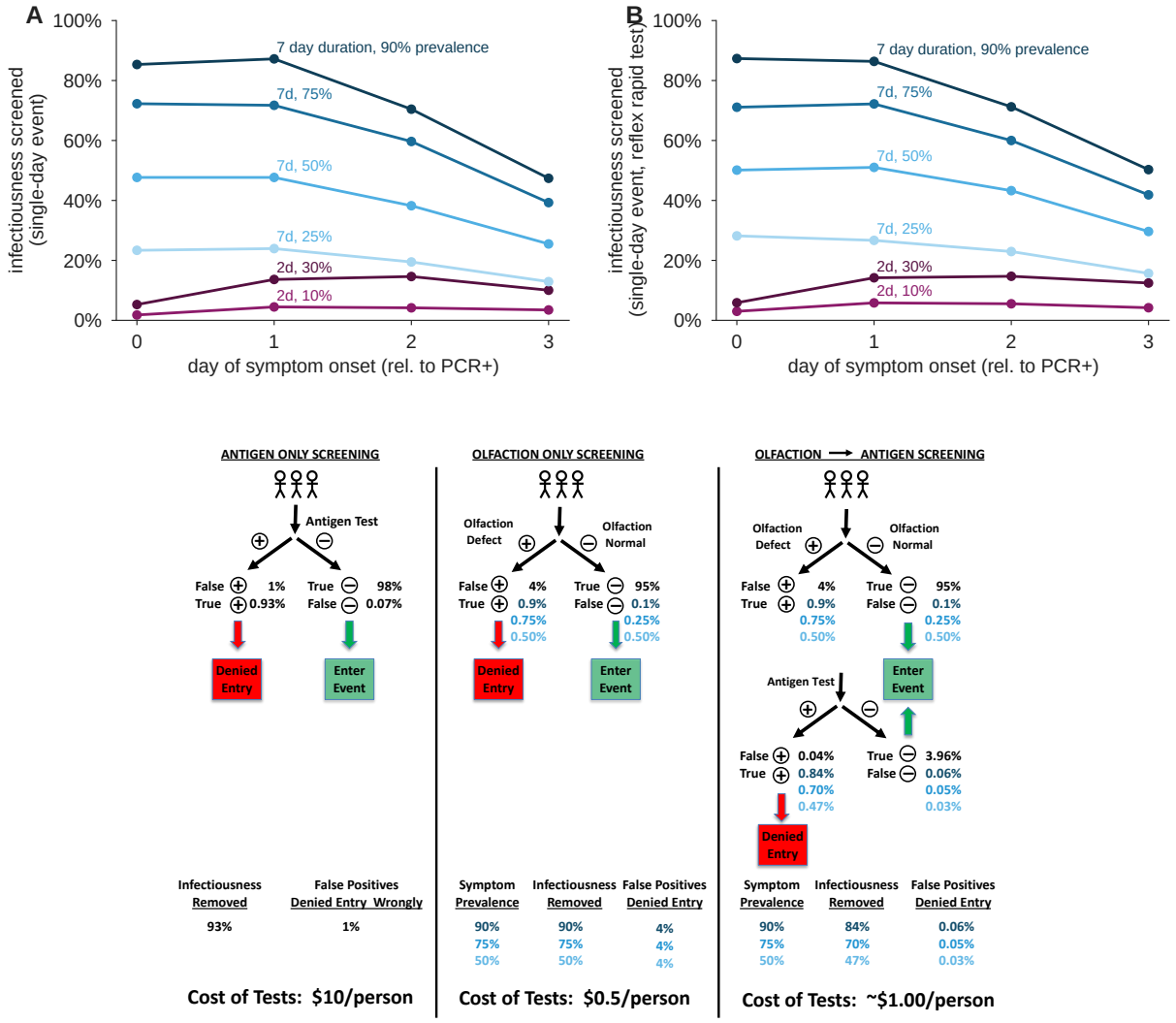

Figure S5: **Olfactory dysfunction and antigen testing for point-of-entry screening.** (A,B) Lines show infectiousness screened for various combinations of symptom prevalence, duration, and onset, without (A) and with (B) reflex testing of those who fail the olfactory test with a rapid antigen test. Blue lines model olfactory dysfunction: 90% (dark blue), 75% (medium blue), 50% (light blue). Red lines model fever: 30% (dark red), 10% (light red). d, duration of symptom in days. (C) Diagram shows the impact of using both olfactory tests and rapid antigen tests in a low-cost but highly effective point-of-entry screening scenario. Symptom onset is assumed to occur one day after viral loads 1000 copies/ml.

medRxiv preprint doi: https://doi.org/10.1101/2020.11.30.20241174; this version posted December 2, 2020. The copyright holder for this preprint (which was not certified by peer review) is the author/funder, who has granted medRxiv a license to display the preprint in perpetuity. It is made available under a CC-BY-NC-ND 4.0 International license .

Supplemental Text

S1 Predicting the impact of repeated population screening testing on R

The impact of repeated population screening on the reproductive number can be estimated by considering the ratio of population infectiousness with a screening regimen to population infectiousness with no screening. However, note that the impact of a population screening policy may depend on two additional factors.

First, not all individuals may wish to participate in a testing program. Let the fraction of individuals who participate be given by ϕ.

Second, a virological test (e.g. RT-PCR) may produce a false negative result *unrelated* to its limit of detection—for instance due to an improperly collected sample. Let se be the test sensitivity, in the particular sense of the probability of correctly diagnosing an individual as positive when that person's viral load should, in principle, have provided a sufficiently high RNA concentration to be detectable.

Let f_0 be the total infectiousness removed with no testing policy, i.e. due to symptom-driven self isolation. Let $f_{\text{test}}(se)$ be the fraction of total infectiousness removed with a chosen testing policy, inclusive of symptom-driven self isolation, as well as the test sensitivity se introduced above. The quantity f_{test} may be computed for any screening program, including virological testing or symptom screening.

Both f_0 and $f_{\text{test}}(se)$ can be estimated rapidly via Monte Carlo by drawing trajectories and applying a population screening regimen to them in which a fraction $1 - se$ positive tests are discarded uniformly at random. In the main text, we found that estimating these values using $10,000$ randomly drawn trajectories was sufficient to produce stable estimates.

Under the assumption of statistical independence between an individual's participation or refusal, viral load or olfactory dysfunction status, and se, we can approximate the reproductive number as

$$R \approx \left[\phi \frac{1 - f_{\text{test}}(se)}{1 - f_0} + 1 - \phi\right] R_0 \,, \tag{S1}$$

which simply expresses a weighted combination of removed infectiousness via screening regimen participation and no test. Intuitively, note that if there is complete refusal to participate ($\phi = 0$) or an entirely ineffective test ($f_{\text{test}}(se) = f_0$), then $R \approx R_0$, as expected.